Advances in Bamboo Science 16 (2026) 100252

Contents lists available at ScienceDirect

Advances in Bamboo Science

journal homepage: www.journals.elsevier.com/advances-in-bamboo-science

Influence of slenderness ratio and eccentricity on the load-bearing capacity of laminated bamboo lumber (LBL) columns derived from *Bambusa spinosa* Roxb

Franklyn Manggapis [a,*], Joe Robert Paul Lucena [b,c], Sanjie Dutt Kumar [d], Aaron Paul Carabbacan [e], Patrick Owen Alimuin [f], Dhan Paul Prietos [d], Harvey Ian Aquino [g]

[a] *Civil Engineering Department, Far Eastern University Alabang, Philippines*
[b] *School of Engineering, Asia Pacific College, Philippines*
[c] *Naveen Jindal Young Global Research Fellowship, O.P. Jindal Global University, India*
[d] *Research and Development Services, Technological University of the Philippines - Taguig, Taguig, Philippines*
[e] *Civil Engineering Department, Colegio de Muntinlupa, Philippines*
[f] *Civil Engineering Department, Emilio Aguinaldo College, Cavite, Philippines*
[g] *Civil Engineering Department, National University, Manila, Philippines*

ARTICLE INFO

Keywords:
Laminated bamboo lumber
Bambusa spinosa
Slenderness ratio
Eccentric loading
Load-bearing capacity

ABSTRACT

Sustainable structural options are needed as conventional materials face supply and carbon constraints. We examined laminated bamboo lumber (LBL) columns manufactured from *Bambusa spinosa* (*kawayang tinik*) and quantified how the slenderness ratio (λ) and eccentricity-to-height ratio (e_o/h) affected the ultimate capacity under eccentric compression. The mechanical properties used in the analysis were parallel to grain. Prismatic LBL columns (50 ×50 and 25 ×25 mm; clear heights, 300, 450, 600 mm) were tested under quasi-static displacement control (0.5 mm min^{-1}). Axial load, including prescribed eccentricities, was introduced through bonded steel end brackets that provided uniform bearing and pinned-like end conditions; offsets were verified prior to loading. There was a clear inverse relation between λ and capacity, reflecting increased buckling susceptibility with slenderness, and a pronounced sensitivity to e_o/h consistent with combined compression–bending. Based on the dataset, a species-specific empirical equation is proposed that integrates λ and e_o/h. Predictions clustered near the identity line with MAE = 1.35 kN, RMSE = 1.69 kN, and MAPE = 9.09% over the tested range (approximately $\lambda \approx 21 - 83$; $e_o/h \approx 0.042 - 0.167$), exhibiting a small conservative bias desirable for design. A benchmark against a published model indicated comparable accuracy while preserving local calibration to *B. spinosa*. In contrast to prior LBL studies that largely feature *Phyllostachys pubescens* and single-eccentricity tests, this work provides a dedicated *B. spinosa* dataset, examines multiple eccentricities together with slenderness, and delivers a calibrated, validated capacity model with a stated domain of applicability. The findings offer design-oriented, species-appropriate guidance for the structural use of engineered bamboo in Philippine practice and similar contexts.

1. Introduction

The construction industry faces growing challenges due to the scarcity of conventional building materials and the escalating environmental impact of their production and use. Over-reliance on materials such as timber, steel and concrete has driven significant resource depletion and carbon emissions, spurring the need for sustainable and eco-friendly alternatives (Eberhardt et al., 2019). As a response, alternative construction materials with environmental advantages, such as engineered wood products (Balasbaneh et al., 2022), recycled materials (Soni et al., 2022), and bamboo (Amatosa et al., 2019), have garnered significant attention. Among these alternatives, bamboo has emerged as a promising substitute due to its renewability, rapid growth and favourable mechanical properties (Iroegbu and Ray, 2021). *Bambusa spinosa* Roxb. (formerly known as *Bambusa blumeana* Schult.f.), known locally as *kawayang tinik*, is one of the most abundant bamboo species in

* Corresponding author.
E-mail address: ffmangapis@feualabang.edu.ph (F. Manggapis).

https://doi.org/10.1016/j.bamboo.2026.100252
Received 31 December 2024; Received in revised form 22 June 2026; Accepted 22 June 2026
Available online 24 June 2026

the Philippines. Its wide availability and adaptability to various climates make it a highly accessible resource for sustainable construction. The robust physical properties of the species position it as an ideal candidate for load-bearing applications in both residential and commercial projects (Salzer et al., 2017).

One of the significant challenges in the structural application of bamboo culms lies in their variability, particularly in their cross-sectional dimensions and mechanical properties, which are influenced by bamboo's natural anisotropy and growth conditions. This variability complicates the assessment of bamboo's grading and hinders its broader adoption in standardized construction practices (Lucena and Dela Cruz, 2023). To address these limitations, engineered bamboo products such as glue-laminated bamboo, bamboo scrimber and parallel strand bamboo lumber have been developed, with Laminated Bamboo Lumber (LBL) emerging as a particularly promising innovation (Ameh and Shittu, 2021). LBL combines the mechanical advantages of bamboo with enhanced uniformity, allowing for higher load-bearing capacities, reduced variability and standardized dimensions suitable for precision construction (Y. Wang et al., 2023). Engineered bamboo products such as LBL have demonstrated promising applications in structural elements such as beams, framings and columns, with columns serving as the focus of our research due to their critical role in structural stability.

A column is a fundamental structural element designed to transfer compressive loads from the structure above down to the foundation, thereby ensuring stability and structural integrity. One of the most important parameters in column design is its load-bearing capacity, which determines the ability of the column to withstand axial and lateral forces without failure (Hao et al., 2024). While substantial research has focused on the behaviour of columns under concentric (axially centred) loading, studies addressing their structural response under eccentric loads remain limited (Yan et al., 2019). Eccentric loading, where the line of action of the compressive force is offset from the column's centroid, introduces bending moments and complex, non-uniform stress distributions. This leads to combined axial compression and bending in the column, posing unique challenges in understanding and predicting performance and failure modes. Moreover, there is a notable scarcity of research exploring the combined effects of slenderness ratio (column height relative to its cross-sectional dimensions) and load eccentricity on the load-bearing capacity of LBL columns. Slenderness ratio is known to influence a column's propensity to buckle, and when coupled with eccentric loading, the interaction can significantly affect stability. Given the growing interest in using engineered bamboo as a sustainable construction material, there is a pressing need for reliable design data and models that account for both slenderness and eccentricity in LBL columns.

Recent studies have focused on the effects of slenderness ratio and eccentricity distance on the load-bearing capacity of LBL columns, recognizing their critical role in structural performance. Li et al. (2020) investigated LBL columns under eccentric compression and identified distinct failure modes influenced by the eccentricity ratio, emphasizing the need for reliable analytical models to predict ultimate resistance. Similarly, Liu et al. (2022) explored the relationship between slenderness ratio and axial compression, finding that as slenderness increases, elastic stages shorten, while lateral deflections grow more prominent, reducing load capacity. Jian et al., (2023) extended this analysis by incorporating BFRP reinforcement in LBL columns, showing improved performance under varying eccentricities but also highlighting challenges in scaling these findings for unreinforced columns. C. Wang et al. (2018) conducted a comparative study of axial and eccentric compression in LBL columns, demonstrating that eccentricity significantly reduces ultimate load capacity and amplifies lateral deflection. Li et al. (2016) explored slenderness effects on stability, reporting that higher slenderness ratios exacerbate buckling failures and lateral deflections, necessitating refined stability equations (Li et al., 2016). Lastly, Chen et al. (2020) highlighted the interplay of slenderness and eccentricity in determining stress-strain behaviour, proposing simplified predictive models that align well with experimental results, whereas prior investigations on LBL columns, predominantly involving *Phyllostachys pubescens* (Carrière) J.Houz. and often a single initial eccentricity, proposed relations for eccentric capacity (Zhou et al., 2022). However, it must be noted that the findings of (Chen et al., 2020) and (Zhou et al., 2022) are not directly transferable to *B. spinosa*, nor to the specific joint variation in slenderness and e_o/h examined here.

Despite these published advances, existing studies lack a comprehensive analysis integrating both slenderness ratio and eccentricity distance as primary variables in predicting the load-bearing capacity of LBL columns, particularly for columns made from *B. spinosa*. Most prior research has focused on isolated aspects either axial vs. eccentric loading or individual effects of slenderness, leaving a significant gap in understanding the combined effect of slenderness and eccentric loading on LBL column performance. This gap in knowledge means that structural engineers currently do not have robust, empirically based guidelines to confidently design LBL bamboo columns for cases where both slenderness and eccentric loading are considerations. The primary problem this paper addresses, therefore, is the lack of empirical data and predictive models that account for how slenderness and eccentricity together influence the ultimate load capacity and failure behaviour of *B. spinosa* LBL columns.

Addressing these gaps, we develop a species-specific experimental dataset for LBL columns fabricated from *B. spinosa* (*kawayang tinik*). We examine multiple eccentricity levels and treat the eccentricity-to-height ratio (e_o/h) together with slenderness to clarify their combined effects; and we propose a single empirical capacity equation that integrates these parameters. The model is calibrated and validated against the experimental results within stated validity ranges, and the findings are distilled into design guidance applicable to Philippine practice and comparable supply chains.

The working hypothesis was that slenderness ratio and load eccentricity jointly and adversely affect the load-bearing capacity of *B. spinosa* LBL columns. Columns with higher slenderness and/or larger eccentricity (greater load offset relative to height) were expected to exhibit lower ultimate capacities and more pronounced lateral deflections than stockier, concentrically loaded counterparts, owing to increased susceptibility to buckling and bending-induced failure. Consistent with this hypothesis, an empirical relation for ultimate load was formulated that explicitly incorporates slenderness and e_o/h and which shows close agreement with measured capacities, with no statistically significant differences within the calibrated domain. The resulting equation provides a practical tool for the safe and efficient design of LBL columns under eccentric compression in the local context.

2. Methodology

Fig. 1 shows the experimental programme of the study; this consists of three main phases: Material preparation, experimental investigation and development of load-bearing capacity formula. Phase 1 involved the selection of materials, fabrication of LBL and the determination of its dimensions and orientation. Phase 2 focused on the characterization of physical and mechanical properties of LBL, designing specimen configurations and conducting experimental tests to obtain data on load-bearing capacity and modes of failure. Finally, Phase 3 entailed analyzing and interpreting the experimental data, developing a formula for load-bearing capacity and comparing calculated and experimental results to validate the findings.

2.1. Phase 1: material preparation

2.1.1. Bamboo species selection and qualification

We selected *B. spinosa*, commonly known as "*kawayang tinik*", for this study based on two major criteria. First, the species is abundant and readily available in the Philippines, ensuring that the material is easily obtainable. Second, the species meets the minimum properties required

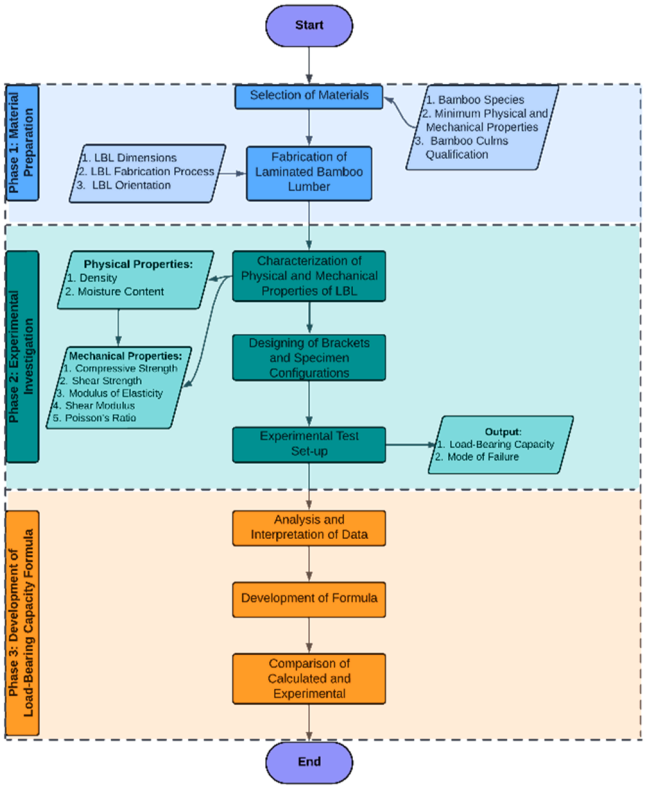

Fig. 1. Research methodology flow diagram.

for structural applications in low-rise construction in the Philippines (Salzer et al., 2017). The selected properties are detailed in Table 1.

We identified bamboo culms for harvesting, ensuring the culms were three to five years old. Maturity was assessed in the field using morphological indicators as chronological records were unavailable. Culms classified as mature (≈3–4 years) were selected based on: (i) dull green to yellow-green colour with reduced sheen; (ii) fully developed, weathered sheath-scar rings and absence of attached green sheaths; (iii) fully developed branching at mid-height; (iv) minimal surface biogrowth indicative of over-aged culms; (v) a higher-pitched tap sound and greater resistance to a light knife scratch; and (vi) internode length/diameter within the mature range observed at the site. Two assessors screened each culm, and only culms meeting all criteria were harvested. The basal section of each culm, extending 3.0 m from the ground level, was harvested for fabrication. This region was selected to ensure a minimum culm diameter of 40 mm and a wall thickness of at least 5 mm, which are critical for LBL production. The harvesting process and cutting into strips are shown in Fig. 2.

2.1.2. Fabrication of laminated bamboo lumber columns

2.1.2.1. Determination of dimension of LBL columns. The dimension of the columns was determined based on the computed critical slenderness ratio, as specified by Eq. (1):

Table 1
Minimum values for various properties required for bamboo used in low-rise construction.

Property	Symbol	Value
Compression strength	f_c	20 ***MPa***
Shear strength	f_v	5 ***MPa***
Modulus of elasticity – 5th percentile	$E_{0.05}$	7400 ***MPa***
Density	ρ_{mean}	570 kg/m^3

Source: (Salzer et al., 2017)

$$\lambda_{cr} = \pi\sqrt{\frac{E_c}{f_c}} \geq 17 \tag{1}$$

Source: (Huang et al., 2015)

where λ_{cr} is the critical slenderness ratio, E_c is the modulus of elasticity in MPa, and f_c is the compressive strength in MPa.

A review of the physical and mechanical properties of engineered bamboo products (Manggapis, Dela Cruz, 2024) reported that the minimum modulus of elasticity parallel to the grain, $E_{\parallel}$ is 8,525 MPa while the minimum compressive strength parallel to the grain, $f_{c_{\parallel}}$ is around 51 MPa. Pre-test estimates of material properties were used only to guide initial sizing. The geometric slenderness classes adopted, and the experimental results reported, were independent of those preliminary values. Substituting these values into Eq. (1), the critical slenderness ratio was computed according to Eq. (2):

$$\lambda_{cr} = \pi\sqrt{\frac{E_c}{f_c}} = \pi\sqrt{\frac{8,525\ MPa}{51\ MPa}} = 40.62 > 17 \tag{2}$$

Eqs. (3)–(5) were used to determine the LBL's moment of inertia, area and radius of gyration, respectively:

$$I_x = \frac{bh^3}{12} \tag{3}$$

$$A_{LBL} = bh \tag{4}$$

$$r = \sqrt{\frac{I_x}{A_{LBL}}} \tag{5}$$

where I_x is the moment of inertia in $\mathbf{mm^4}$, A_{LBL} is the cross-sectional area of LBL in $\mathbf{mm^2}$, b is the width of LBL in **mm**, h is the thickness of LBL in **mm**, and r is the radius of gyration in **mm**.

The actual slenderness ratio was determined by Eq. (6) to set the total length of the column:

$$\lambda_{act} = \lambda_{cr} = \frac{L}{r}; L = \lambda_{cr} r \tag{6}$$

Based on Eq. (6), the selected dimensions and configurations for the study were obtained as shown in Table 2. Test members were LBL prisms with nominal cross-sections of 50 × 50 mm and 25 × 25 mm and clear heights of 300, 450 and 600 mm, measured between the end-bracket bearing faces. Finally, four configurations were formulated for fabrication of the LBL test specimen, as shown in Table 3.

2.1.2.2. Fabrication process for the LBL columns. Bamboo culms were cut into strips 5 mm× 5 mm for configuration 1, and 10 mm× 5 mm for configuration 2. Prior to lamination, the strips were soaked in saline water for seven days and air-dried for seven days to reduce the risk of biodeterioration during handling. Saline soaking is used to leach water-soluble sugars/starches that attract borers and to leave saline residues that are less hospitable to insects and fungi; its application to laminated bamboo composites has been documented in prior work (Amatosa et al., 2019). The lamination followed immediately after drying. Culms were split into strips (lamellae) and planed to remove nodal diaphragms; strips showing pronounced node remnants, voids or defects were rejected. The final lay-up therefore contained no continuous nodal ring, and any minor residual features were dispersed across plies.

The strips were glued and pressed using a pressing machine until the desired dimensions were achieved. Strips were bonded using a structural melamine–urea–formaldehyde (MUF) adhesive (resin: hardener 100:20 by mass). Bond faces were planed, lightly sanded and cleaned of dust before a double-spread application at a typical structural rate, with closed assembly within about 10 min. Lamination was hot-pressed at approximately 1 MPa and 110 °C for about 20 min, after which members were kept under restraint until cool. Lamella moisture content at

Fig. 2. Harvesting and cutting bamboo processes.

Table 2
Calculated dimensions of the LBL materials.

Properties	Configuration #1	Configuration #2
Cross-sectional dimension, **mm**	25 × 25	50 × 50
Area, **mm²**	625	2500
Moment of inertia, **mm⁴**	32,552,08	520,0833.33
Radius of gyration, **mm**	7.2169	14.4338
Length, **mm**	293.15 ≈ 300	586.30 ≈ 600

Table 3
LBL specimen label, slenderness ratio, and eccentric distance over height ratio.

Specimen	Specimen ID	Slenderness ratio (λ)	Eccentric distance (e_o), **mm**	Eccentric distance over height ratio, (e_o/h)
LBL50x50x300	LBL50x50x300–1 LBL50x50x300–2 LBL50x50x300–3	20.78	50	0.1667
LBL50x50x450	LBL50x50x450–1 LBL50x50x450–2 LBL50x50x450–3	31.18	50	0.0111
LBL50x50x600	LBL50x50x600–1 LBL50x50x600–2 LBL50x50x600–3	41.57	50	0.0833
LBL25x25x300	LBL25x25x300–1 LBL25x25x300–2 LBL25x25x300–3	41.57	25	0.0833
LBL25x25x450	LBL25x25x450–1 LBL25x25x450–2 LBL25x25x450–3	62.35	25	0.0556
LBL25x25x600	LBL25x25x600–1 LBL25x25x600–2 LBL25x25x600–3	83.14	25	0.0417

bonding was approximately 10–12%. Following pressing, members were conditioned at ~20 °C and ~65% RH for seven days prior to machining and testing. Bond quality was checked visually (continuous glue lines, squeeze-out, no delamination) and by spot block-shear on off-cuts to confirm satisfactory adhesive performance. This process ensured the production of high-quality laminated bamboo columns suitable for thorough experimental investigation. The finished process is shown in Fig. 3.

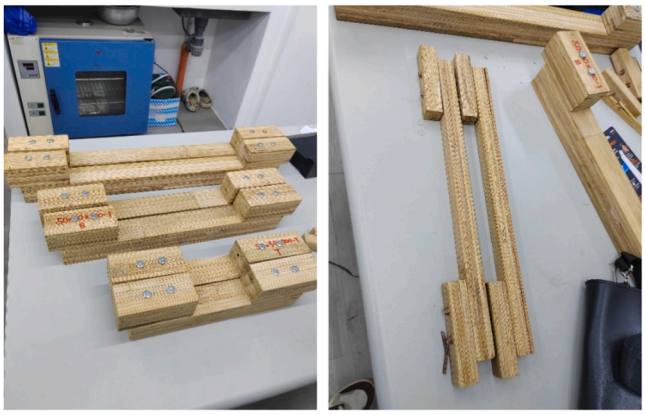

Fig. 3. The fabricated laminated bamboo lumber.

2.1.2.3. Orientation of LBL columns. Primarily there are three main directions for LBL columns, shown in Fig. 4. Longitudinal direction (L) corresponds to the axis parallel to the length of the bamboo strips, tangential direction (T) lies along the width of the strips and radial direction (R) lies along the thickness of the strips. For the easiness of the direction, a number will represent the direction accordingly: 1 – (L) for longitudinal direction; 2 – (T) for tangential direction; and 3 – (R) for radial direction.

2.2. Phase 2: Experimental investigation

We characterized the properties of the LBL columns to provide a comprehensive understanding of the behaviour of this material, with the values being used for the preliminary definition of the material characteristics. The process involved both physical and mechanical testing, adhering to ASTM D143–21: Standard Test Methods for Small Clear Specimens of Timber (ASTMD143). The dimensions of the LBL specimens were prepared in accordance with ASTM D143, as shown in Table 4.

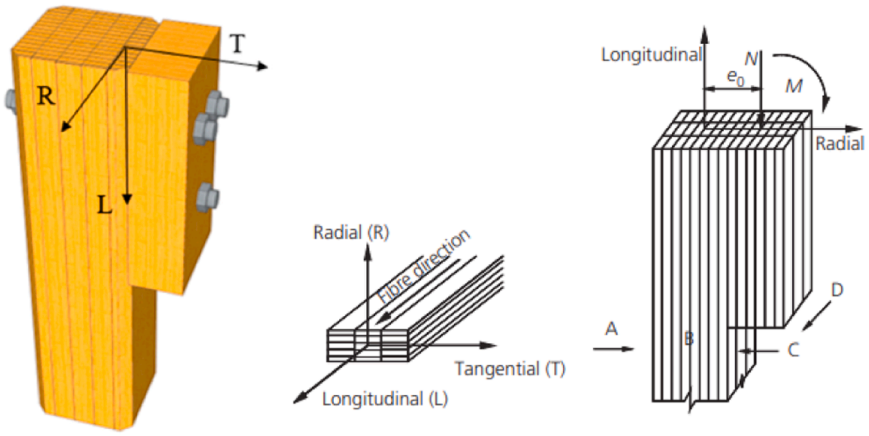

Fig. 4. Main directions of LBL columns. Source: (Hong et al#, 2021; Li, Liu, et al#, 2019).

Table 4
ASTM D143 Standard testing.

ASTM D143 Section #	Properties	Dimension
3	Unit weight and moisture content	50 mm× 50 mm× 50 mm
9	Compression strength test	50 mm× 50 mm x 200 mm
14	Shear strength test	50 mm x 50 mm x 63 mm

2.2.1. Determination of LBL physical and mechanical properties

2.2.1.1. Determination of LBL density and moisture content. The unit weight of the LBL specimens was determined to assess the density and mass per unit volume, which is critical for understanding the material's load-bearing capacity. The samples were carefully measured for volume and mass, and the density was calculated using Eq. (7):

$$\gamma_{LBL} = \frac{M_{LBL}}{V_{LBL}} \tag{7}$$

where $\boldsymbol{M_{LBL}}$ is the mass of the LBL in **kg**, $\boldsymbol{V_{LBL}}$ is the volume of LBL in $\mathbf{mm^3}$, and γ_{LBL} is the density of LBL in $\mathbf{kg/m^3}$.

The moisture content of the LBL was measured using the oven-dry method prescribed in ASTM D143. This involved weighing the specimens before and after drying in an oven at a specified temperature until a constant weight was achieved, as depicted in Fig. 5. The moisture content was calculated using Eq. (8):

$$\boldsymbol{MC} = \frac{\boldsymbol{M_{bulk}} - \boldsymbol{M_{dry}}}{\boldsymbol{M_{bulk}}} \tag{8}$$

Where $\boldsymbol{M_{bulk}}$ is the bulk mass of the LBL in **kg**, $\boldsymbol{M_{dry}}$ is the dried mass of LBL in **kg**, *MC* is the moisture content of the specimen in %.

2.2.1.2. Determination of LBL compressive strength and modulus of elasticity. The compressive stress-strain diagram was plotted for each group for the modulus of elasticity in the three directions of LBL ($\boldsymbol{E_1}$, $\boldsymbol{E_2}$, $\boldsymbol{E_3}$), by obtaining the initial slope of the curve. Three groups of test specimens were tested in compression as shown in Fig. 6, each corresponding to the compressive strength along different directions: $\bar{\sigma}_{11}$, (longitudinal), $\bar{\sigma}_{22}$ (tangential), and $\bar{\sigma}_{33}$ (radial). A constant cross-head rate of 1.0 mm/min was used, targeting a 3–10 min time to failure

Fig. 6. Compressive strength test for LBL specimen.

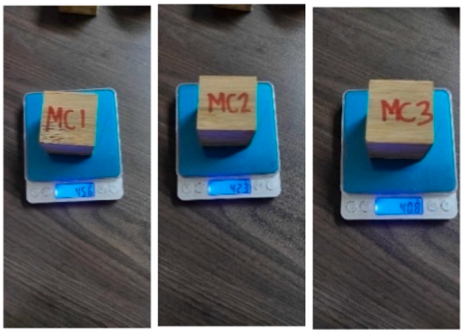

Weighing of laminated bamboo

Oven-drying of laminated bamboo

Fig. 5. Moisture content determination of laminated bamboo lumber.

windows. The load at specimen failure was recorded, and the yielding compressive strength was obtained using Eq. (9).

$$\bar{\sigma}_{ii} = \frac{P}{bt} \quad (i = 1, 2, 3) \tag{9}$$

where P is the maximum load at failure of the LBL specimen in kN, b is the width of LBL in mm, t is the thickness of LBL specimen in mm, and $\bar{\sigma}_{ii}$ is yielding compressive strength in MPa.

2.2.1.3. Determination of LBL shear strength and shear modulus of elasticity. The shear stress-strain diagram was plotted for each group for the shear modulus of elasticity in the three directions of LBL (G_{12}, G_{13}, G_{23}), by obtaining the initial slope of the curve. Three groups of specimens were tested for shear strength as depicted in Fig. 7, each corresponding to different planes of LBL: τ_{12} (longitudinal-tangential), τ_{13} (longitudinal-radial), and τ_{23} (tangential-radial). The load with a constant rate of 1.0 mm/min at specimen failure was recorded, and the yielding shear strength was computed using Eq. (9):

$$\bar{\tau}_{ij} = \frac{P}{bt} \ (i = 1, 2, 3 | \ j = 1, 2, 3) \tag{9'}$$

where P is the maximum load at failure of the LBL specimen in kN, b is the width of LBL in mm, t is the thickness of LBL specimen in mm, and $\bar{\tau}_{ij}$ is yielding shearing strength in MPa.

2.2.2. Design of brackets and specimen configuration

To introduce eccentric compression during testing, customized end brackets were attached to the top and bottom ends of each LBL column. Each bracket was fixed to the column using two self-tapping screws. The bracket was intentionally positioned so that part of it protruded beyond the column face, allowing the plate of the universal testing machine to apply the compressive load away from the centroidal axis of the column.

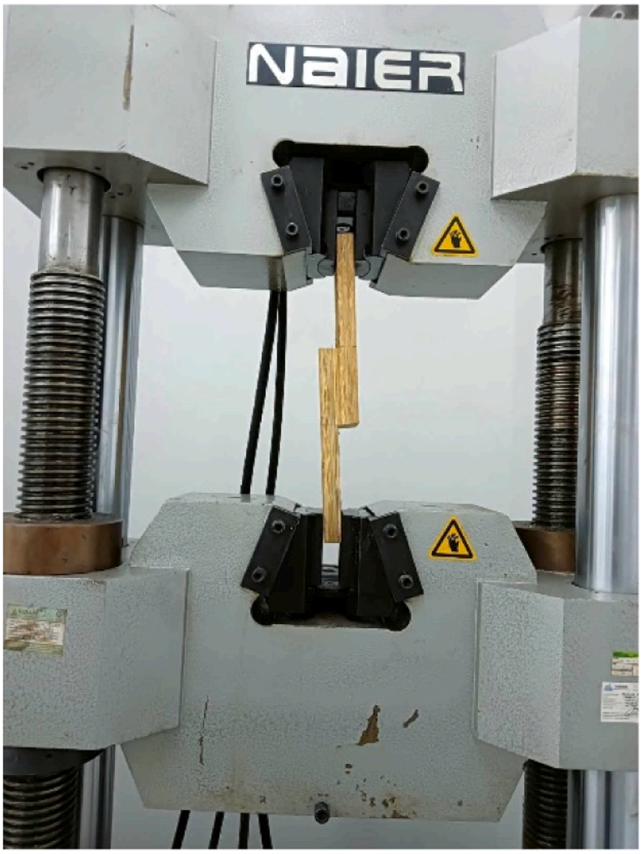

Fig. 7. Shear strength test for LBL specimen.

This offset created the required eccentricity and induced combined axial compression and bending in the specimen. The customized bracket configuration used in the experiment is shown in Fig. 8. The general eccentric-loading concept was inspired by previous studies on laminated bamboo columns under eccentric compression (Hong et al., 2021); however, the bracket configuration used in this study was specifically designed and fabricated by the authors for the available testing setup.

2.3. Test configuration

Four groups of LBL columns were transferred to the INCH-ON Materials Testing Laboratory in Quezon City for testing. The schematic test configuration is shown in Fig. 9(a), and the real-life test setup is shown in Fig. 9(b). Both ends of LBL columns were supported with unidirectional hinges to ensure the specimen could only rotate in the eccentric load direction. Column tests were run under quasi-static displacement control at a constant crosshead rate of 0.5 mm/min after a short seating preload and 60-s hold; loading continued without interruption until peak load and subsequent drop (failure) The failure modes were also observed and documented.

2.4. Phase 3: comparison and development of formula

The final phase focused on analyzing and interpreting the data collected during the experimental phase to derive a mathematical formula for predicting the load-bearing capacity of laminated bamboo bumber (LBL) columns. This phase involved identifying key parameters such as slenderness ratio and eccentric distance, which influence column behaviour under load. The developed formula was then calibrated and refined by comparing its predictions with the experimental results to ensure accuracy and reliability. By bridging experimental findings with theoretical modeling, this phase laid the groundwork for creating a practical design tool for structural applications of LBL columns.

3. Results and discussion

3.1. Physical properties of LBL

3.1.1. Mass density

The physical properties of LBL columns were evaluated to understand their density and moisture content, essential factors affecting their structural performance. The density of the LBL samples was calculated by measuring their volume and weight. The findings showed that the average density of the LBL columns was 743.33 kg/m^3 , as shown in Table 5, consistent with earlier research on bamboo-based materials.

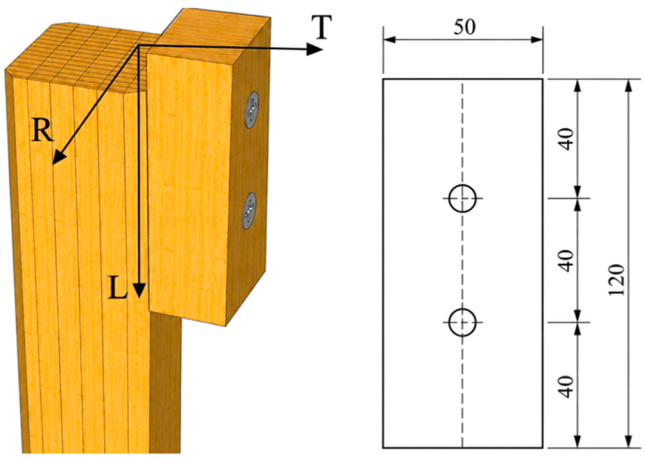

Fig. 8. Customized protruding end-bracket system used to introduce eccentric compression in the LBL column specimens.

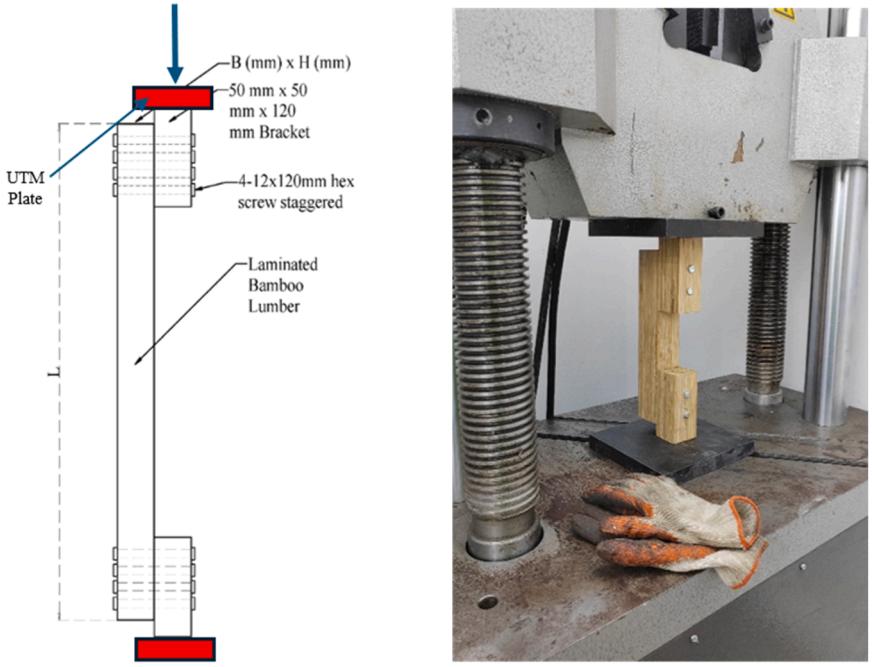

Fig. 9. (a) Schematic test configuration, and (b) Laboratory test configuration.

Table 5
Density of laminated bamboo lumber.

Specimen ID	Density (kg/m^3)	Mean (kg/m^3)	Standard deviation (kg/m^3)	COV (%)
LBL-MD−1	743.2	743.68	0.70	0.09
LBL-MD−2	742.3			
LBL-MD−3	744.5			

3.1.2. Moisture content

Moisture content, a vital factor affecting mechanical properties, was measured using the oven-dry method prescribed in ASTM D143. Specimens were weighed before and after drying in an oven until a constant weight was achieved. The average moisture content was 8.30% (Table 6), highlighting the material's stability under varying environmental conditions. These findings provide a comprehensive understanding of the LBL's physical properties, essential for predicting its behaviour under load.

3.2. Mechanical properties of LBL

3.2.1. Compressive strength

The mechanical properties of LBL columns were characterized to understand their behaviour under various loading conditions. The compressive strength tests (Table 7), revealed that the average compressive strengths were 63.70 MPa, 24.74 MPa, and 21.92 MPa for the longitudinal ($\bar{\sigma}_{11}$), tangential ($\bar{\sigma}_{22}$) and radial ($\bar{\sigma}_{33}$), directions, respectively.

Table 6
Moisture content of laminated bamboo lumber.

Specimen ID	Moisture content (%)	Mean (%)	Standard deviation (%)	COV (%)
LBL-MC−1	8.23	8.30%	0.220	2.758
LBL-MC−2	8.56			
LBL-MC−3	8.12			

Table 7
LBL compressive strength along three directions.

Parameters	Specimen ID	Compressive strength (MPa)	Mean (MPa)	Standard deviation (MPa)	COV (%)
$\bar{\sigma}_{11}$	CS11–1	64.29	63.70	1.435	2.25
	CS11–2	62.06			
	CS11–2	64.74			
$\bar{\sigma}_{22}$	CS22–1	24.21	24.74	0.839	3.39
	CS22–2	24.31			
	CS22–2	25.71			
$\bar{\sigma}_{33}$	CS33–1	24.22	21.93	2.29	10.44
	CS33–2	19.64			
	CS33–2	21.93			

3.2.2. Modulus of elasticity

Fig. 10 (a) displays the combined compressive stress-strain curves for all LBL columns. The modulus of elasticity in each direction was determined by calculating the initial slope of the respective stress-strain curves. Fig. 10 (b) – (d) show the mean modulus of elasticity curves for the longitudinal, tangential and radial directions. The average moduli of elasticity were $\boldsymbol{E_1 = 4,793.87MPa}$, $\boldsymbol{E_2 = 1,342.92MPa}$, and $\boldsymbol{E_1 = 1,377.87MPa}$ for the longitudinal, tangential and radial directions, respectively. These values reveal the material's stiffness and its capacity to deform elastically under load, offering essential insights into the structural performance of the LBL columns.

3.2.3. Shear strength

For the shear strength tests, the laminated bamboo specimens were subjected to a shear adhesive-bond test. The maximum load sustained by each specimen prior to failure was recorded and used to calculate the shear strength by dividing the failure load by the corresponding bonded area. Hong et al. (2021) found that the shear strength in a longitudinal-tangential direction ($\bar{\tau}_{12}$) was almost equal to the shear strength in a longitudinal-radial direction ($\bar{\tau}_{13}$), and this was applied in this study, while the shear strength in a tangential-radial direction ($\bar{\tau}_{23}$) was based on the study by Yang et al. (2020). Table 8 shows the shear

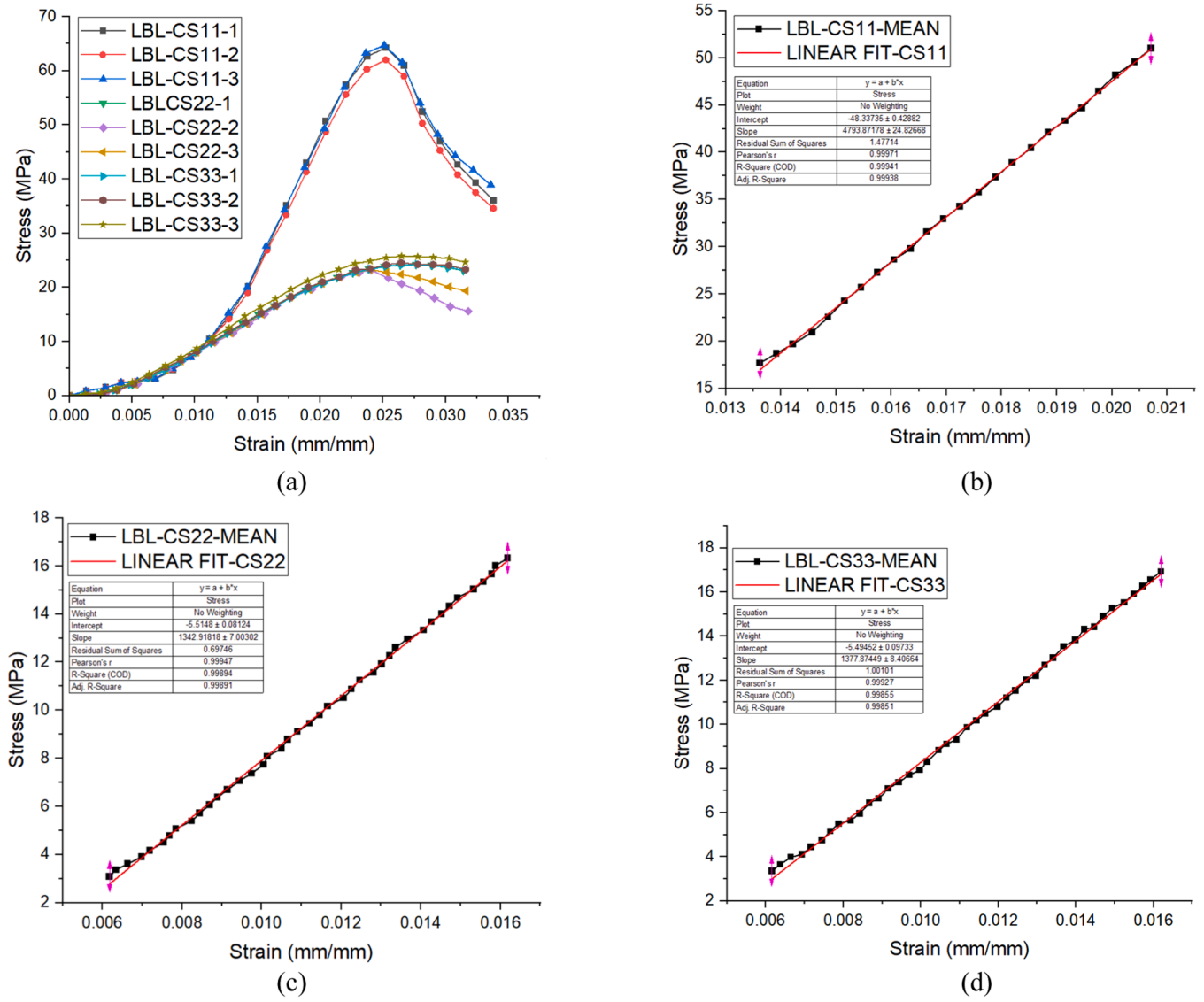

Fig. 10. (a) Compressive strain-stress diagram in all directions of LBL, (b) modulus of elasticity of LBL in the longitudinal direction, (c) modulus of elasticity of LBL in the tangential direction, and (d) modulus of elasticity of LBL in the radial direction.

Table 8
LBL Shear strength in various directions.

Parameters	Specimen ID	Shear strength (MPa)	Mean (MPa)	Standard deviation (MPa)	COV (%)
$\bar{\tau}_{12}/\bar{\tau}_{13}$	LBL-SS12–13–1	18.19	15.35	2.469	16.09
	LBL-SS12–13–2	13.74			
	LBL-SS12–13–3	14.11			
$\bar{\tau}_{23}$	-	6.00	6.00	-	-

stress test results for the columns. The average shear stress in a longitudinal-tangential/longitudinal-radial direction was 15.35 MPa, while the shear strength in a tangential-radial direction was 6 MPa (Yang et al., 2020). Fig. 11 illustrates the stress-strain diagram in terms of shear strength.

3.2.4. Shear modulus of elasticity

The shear modulus of elasticity was obtained by examining the initial slope of the shear stress-strain diagram and fitting a linear equation to the graph, as shown in Fig. 12. In line with the shear strength concept, the shear modulus in the longitudinal-tangential direction (G_{12}) was the same as in the longitudinal-radial direction (G_{13}). The shear modulus for the tangential-radial direction (G_{23}) was obtained from Yang et al. (2020). Additionally, Poisson's ratios for the LBL were also sourced from Yang et al. (2020). All these values are compiled in Table 9.

3.2.5. Constitutive model parameters

Table 10 provides a comprehensive summary of the constitutive model parameters for laminated bamboo lumber (LBL), including key mechanical properties such as modulus of elasticity, shear modulus, compressive strength, shear strength and Poisson's ratio. The values were derived from both experimental investigations and previous studies, offering the essential orthotropic material properties required for numerical modeling. While not a direct objective of our study, these parameters served as critical inputs for finite element analysis (FEA) to simulate and validate the behaviour of LBL under various loading conditions. By bridging experimental results with numerical models, this table facilitates comparisons that can enhance the understanding of LBL's structural performance and contribute to future research efforts.

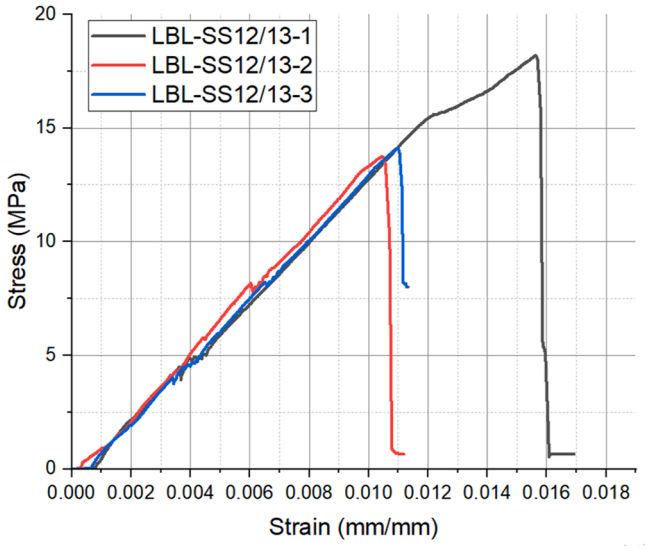

Fig. 11. LBL shear strength in a longitudinal-tangential direction.

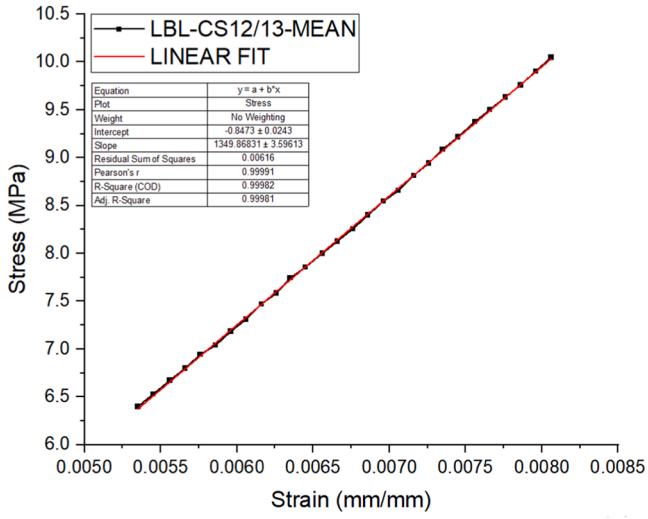

Fig. 12. LBL shear modulus of elasticity in a longitudinal-tangential direction.

Table 9
LBL shear modulus of elasticity and Poisson's ratio.

Parameters	Shear modulus of elasticity (MPa)	Reference	Parameters	Poisson's ratio	Reference
G_{12}	1349.87	Our experiment	ν_{12}	0.25	Hong et al. (2021)
			ν_{21}	0.053	
G_{13}	1349.87	Our experiment	ν_{13}	0.2	
			ν_{31}	0.04	
G_{23}	460.00	Yang et al. (2020)	ν_{23}	0.42	
			ν_{32}	0.42	

3.3. Experimental investigation

3.3.1. Load-bearing capacity results from the experiments

The load-bearing capacity of laminated bamboo lumber (LBL) columns was investigated through a series of eccentric compression tests. These tests evaluated how the slenderness ratio and eccentric distance affect the structural performance of LBL columns. The maximum load in each specimen is shown in Table 11. Fig. 13 illustrates the load-displacement curves for six specimens. These curves depict the relationship between the applied load and the resulting displacement, highlighting the load-bearing capacity and failure characteristics of each specimen.

The load-bearing capacities of LBL columns were affected significantly by their cross-sectional dimensions and length. Specimens with larger cross-sectional areas (50 ×50 mm) demonstrated higher load-bearing capacities and more ductile behaviour compared to smaller cross-sectional specimens (25 ×25 mm). Additionally, the length of the specimens affected the load-bearing capacity, with shorter columns (300 mm) showing higher peak loads and more pronounced post-peak deformations.

3.3.2. Modes of failure

The mode of failure of eccentrically loaded LBL columns was analyzed to understand the structural performance and failure mechanisms of the material. Observations and data collected during the tests provided critical insights into how different specimens behaved under load and the factors influencing their failure modes.

The LBL50x50x300 specimen exhibited a combination of compressive and buckling failures. Initially, the column experienced uniform compressive stress, leading to slight deformations. As the load increased, localized failure was observed at the connections of the bracket on the sample (Fig. 14(a)). This behaviour indicates a complex interaction between material properties and geometry, where the column's shorter length and larger cross-section contributed to a higher load-bearing capacity and a more ductile failure. The LBL50 × 50x450m specimen mode of failure (Fig. 14(b)) revealed a combination of buckling and compressive crushing under eccentric compression loading. The specimen displayed significant lateral deformation indicative of buckling, starting from the mid-height and propagating towards the ends, due to its moderate slenderness ratio. Additionally, compressive crushing at the load application points was evident, with localized crushing and splitting at the top and bottom sections where high stress concentrations led to the material's failure. The failure mode of the LBL50x50x600 specimen (Fig. 14(c)) was characterized primarily by pronounced buckling. The significant lateral deformation along the length of the column indicated a loss of stability under eccentric loading, which was attributed to the specimen's high slenderness ratio. The pronounced curvature and lateral deflection demonstrated the column's inability to withstand the eccentric load, leading to a catastrophic buckling failure.

Failure in the LBL25x25x300 specimen (Fig. 15(a)) was characterized by a combination of compressive crushing and splitting. The short length and large cross-sectional area of the specimen allowed it to withstand higher loads initially, but the high stress concentrations at the points of load application led to localized crushing. The image shows multiple splits and fractures along the length of the column, indicating that the material failed under excessive compressive forces. This dual failure mode highlights the interplay between material strength and geometric dimensions, emphasizing the need for robust design considerations to prevent such failures in structural applications. The LBL25x25x450 specimen exhibited a failure mode that primarily consisted of buckling (Fig. 15(b)). The pronounced curvature along the length of the column indicated significant lateral deformation due to the slenderness of the specimen under eccentric loading. This deformation is a classic sign of buckling failure, where the column loses stability and bends laterally under the applied load. The absence of significant splitting or crushing suggested that the failure was dominated by the instability caused by the slender geometry, emphasizing the critical influence of slenderness ratio on the structural performance of LBL columns. Failure in the LBL25x25x600 specimen (Fig. 15(c)) was characterized by severe buckling. The significant lateral deformation and pronounced curvature along the entire length of the columns indicated a loss of stability under eccentric loading due to the high

Table 10
Summary of LBL's constitutive model parameters.

Modulus of elasticity (MPa)		Shear modulus of elasticity (MPa)		Compressive strength (MPa)		Shear strength (MPa)		Poisson's ratio	
E_1	4793.87	G_{12}	1349.87	$\bar{\sigma}_{11}$	63.70	$\bar{\tau}_{12}$	15.35	ν_{12}	0.25
								ν_{21}	0.053
E_2	1342.92	G_{13}	1349.87	$\bar{\sigma}_{22}$	24.74	$\bar{\tau}_{13}$	15.35	ν_{13}	0.2
								ν_{31}	0.04
E_3	1377.87	G_{23}	460	$\bar{\sigma}_{33}$	21.93	$\bar{\tau}_{32}$	6.00	ν_{23}	0.42
								ν_{32}	0.42

Table 11
LBL eccentric compression test results.

Parameters	Specimen ID	Maximum load (kN)	Mean (kN)	Standard deviation (kN)	COV (%)
50x50x300	LBL50x50x300–1	33.07	35.04	2.507	7.156
	LBL50x50x300–2	34.18			
	LBL50x50x300–3	37.86			
50x50x450	LBL50x50x450–1	31.86	30.14	1.725	5.724
	LBL50x50x450–2	28.41			
	LBL50x50x450–3	30.14			
50x50x600	LBL50x50x600–1	28.69	27.58	1.378	5.00
	LBL50x50x600–2	26.04			
	LBL50x50x600–3	28.02			
25x25x300	LBL25x25x300–1	7.10	6.78	1.013	14.931
	LBL25x25x300–2	5.65			
	LBL25x25x300–3	7.60			
25x25x450	LBL25x25x450–1	4.60	5.25	0.737	14.029
	LBL25x25x450–2	5.10			
	LBL25x25x450–3	6.05			
25x25x600	LBL25x25x600–1	5.61	4.06	1.365	33.642
	LBL25x25x600–2	3.51			
	LBL25x25x600–3	3.05			

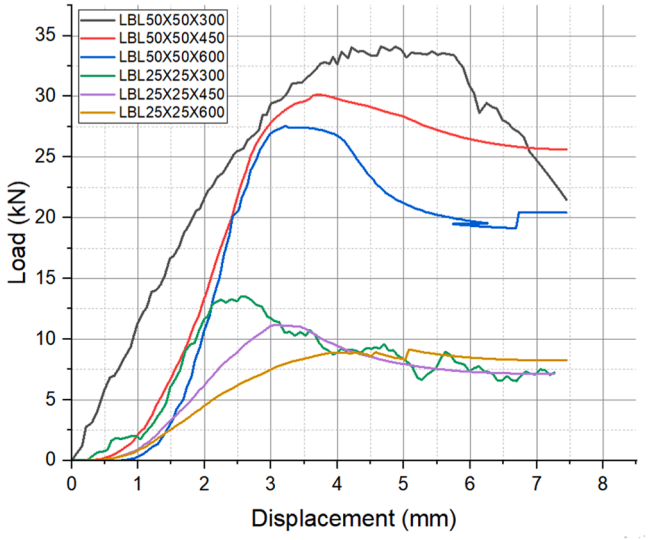

Fig. 13. Eccentric compression load-displacement of LBL samples.

slenderness ratio of the specimen. The bending and bowing observed suggested that the column failed primarily through buckling, with the material unable to resist the lateral forces induced by the eccentric load.

4. Development of an ultimate load-bearing capacity formula

In the formulation of the proposed empirical formula for determining the load-bearing capacity of Laminated Bamboo Lumber, two independent variables had to be taken into consideration: (1) Slenderness ratio (λ), and (2) Eccentricity/height ratio (e_o/h). As the cross-sectional dimension of LBL differs with 50 mm x 50 mm and 25 mm x 25 mm, the stress would be the dependent variable. To determine this, the maximum load obtained in the experimental test in each specimen was divided by its corresponding cross-sectional area. Table 12 illustrates the calculated stress, its slenderness ratio and its corresponding eccentricity/height ratio.

Fig. 16 illustrates the relationship between the stress and the slenderness ratio (λ) for the LBL columns. The data points, represented by black triangles, show the experimental stress values at different slenderness ratios. The red line represents a trend line that captures the general decreasing trend of stress with increasing slenderness ratio. This inverse relationship shows that when the slenderness ratio (λ) increases, the stress capacity of the LBL columns decreases. This trend implies that columns with higher slenderness ratios are more susceptible to buckling under lower stress levels.

Fig. 17 shows the relationship between the stress and the eccentricity over height ratio and the stress (MPa) for laminated bamboo lumber (LBL) columns. The data points, represented by black diamonds, display the experimental stress values at various eccentricity/height ratios. The red line represents a trend line that demonstrates the increasing trend of stress with rising eccentricity/height ratios. This positive relationship indicates that as the eccentricity/height ratio increases, the stress capacity of the LBL columns also increases. This trend suggests that columns subjected to higher eccentricities experience greater stress concentrations, leading to higher stress values.

The observed correlation between slenderness ratio (λ), eccentricity/height ratio (e_o/h), and stress (MPa), is because specimens with lower slenderness ratios tended to exhibit higher stress values, indicating that columns with a smaller slenderness ratio are more capable of resisting higher stresses. Conversely, higher slenderness ratios correlated with lower stress capacities, highlighting the increased susceptibility to buckling under load. Additionally, the eccentricity/height ratio played a significant role. Higher e_o/h ratios were associated with increased stress, suggesting that greater eccentricity led to higher stress concentrations within the column. This interplay between slenderness ratio, eccentricity/height ratio, and stress underscores the importance of optimizing these parameters in the design of LBL columns to enhance their structural performance and stability under eccentric loading conditions.

To understand further the relationship between the variables, the data in Table 12 were plotted on a 3-dimensional spatial surface using OriginPro (Fig. 18). A spatial surface functional model enabled the relationship between the variables to be expressed in Eq. (10):

$$\sigma_{cu} = A + \frac{-B}{\left[1+\left(\frac{\lambda}{C}\right)^{-D}\right]\left[1+\left(\frac{\frac{e_0}{h}}{E}\right)^{-F}\right]} \tag{10}$$

where σ_{cu} is the calculated stress, A to F are coefficients obtained using experimentation, λ is the slenderness ratio, and e_o/h is the eccentricity over height ratio. The coefficients can be obtained by regression analysis, as shown in Eq. (11):

Fig. 14. Modes of failure for 50 × 50 LBL with lengths of: (a) 300 mm, (b) 450 mm, and (c) 600 mm.

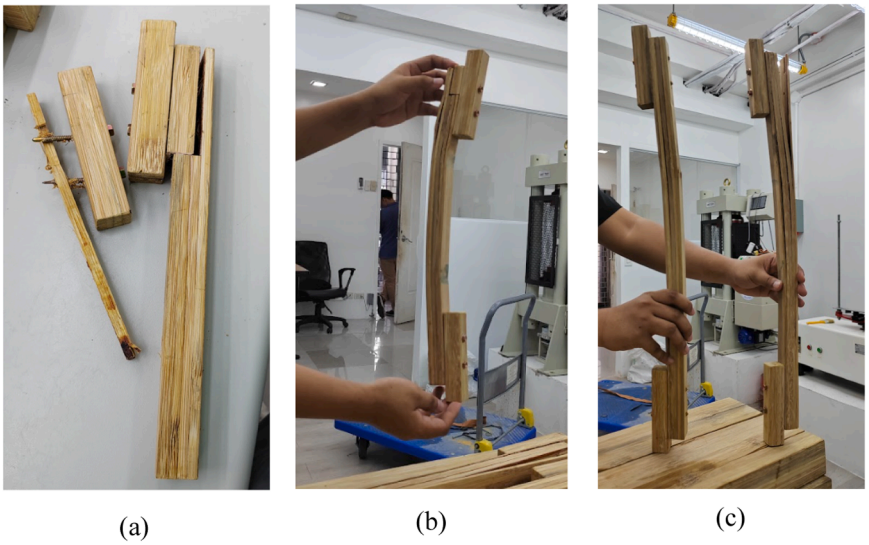

Fig. 15. Modes of failure for 25 x 25 mm LBL with lengths of: (a) 300 mm, (b) 450 mm, and (c) 600 mm.

$$\sigma_{cu} = 15.1 + \frac{-21.7}{\left[1+\left(\frac{\lambda}{40.2}\right)^{-2.8}\right]\left[1+\left(\frac{\frac{e_0}{h}}{0.1}\right)^{-0.5}\right]} \tag{11}$$

To determine the general empirical formula to determine the load-bearing capacity of the LBL column, the expression N_{ul}/A_{LBL} to σ_{cu} was substituted, as shown in Eq. (12). To confirm the reliability of the proposed formula, it was compared with the experimental test results presented in Table 13.

$$N_{ul} = \left\{ 15.1 + \frac{-21.7}{\left[1+\left(\frac{\lambda}{40.2}\right)^{-2.8}\right]\left[1+\left(\frac{\frac{e_0}{h}}{0.1}\right)^{-0.5}\right]} \right\} (A_{LBL}) \tag{12}$$

The scatter in Fig. 19 indicates good agreement between the proposed equation and the test results. The data cluster close to the $y = x$ line, with all deviations within ±3.5 kN. Errors were slightly negative

Table 12
Experimental investigation of stress results.

Parameters	Specimen ID	λ	e_o/h	Stress (MPa)
50x50x300	LBL50 × 50x300–1	20.7846	0.1667	13.23
	LBL50 × 50x300–2	20.7846	0.1667	13.67
	LBL50x50x300–3	20.7846	0.1667	15.14
50x50x450	LBL50x50x450–1	31.1769	0.1111	12.74
	LBL50x50x450–2	31.1769	0.1111	11.36
	LBL50x50x450–3	31.1769	0.1111	12.06
50x50x600	LBL50x50x600–1	41.5692	0.0833	11.48
	LBL50x50x600–2	41.5692	0.0833	10.42
	LBL50x50x600–3	41.5692	0.0833	11.21
25x25x300	LBL25x25x300–1	41.5692	0.0833	11.36
	LBL25x25x300–2	41.5692	0.0833	9.04
	LBL25x25x300–3	41.5692	0.0833	12.16
25x25x450	LBL25x25x450–1	62.3538	0.0556	7.36
	LBL25x25x450–2	62.3538	0.0556	8.16
	LBL25x25x450–3	62.3538	0.0556	9.68
25x25x600	LBL25x25x600–1	83.1384	0.0417	8.98
	LBL25x25x600–2	83.1384	0.0417	5.62
	LBL25x25x600–3	83.1384	0.0417	4.88

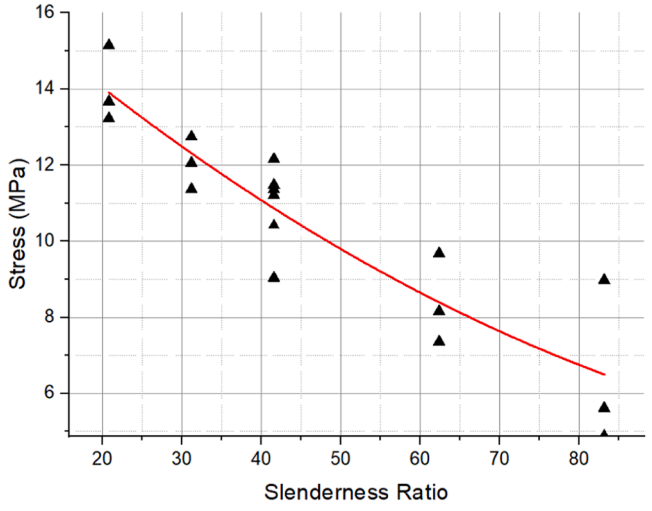

Fig. 16. Slenderness ratios-stress diagram.

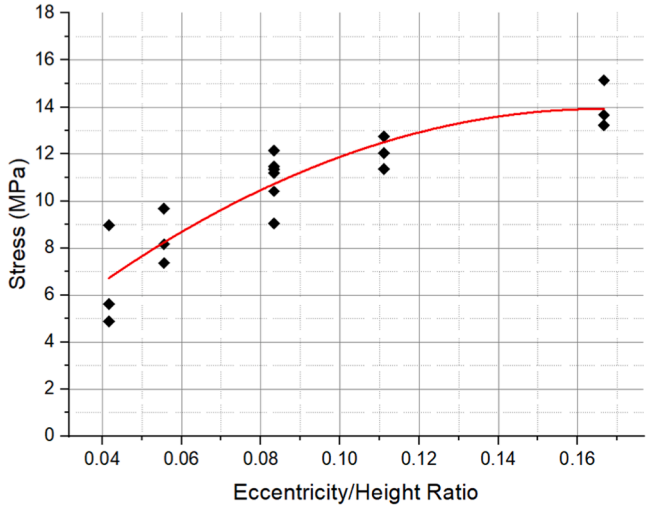

Fig. 17. Eccentric distance over height ratio-stress diagram.

on average (Bias = −1.13 kN), reflecting modest under-prediction for the 50 × 50 series; the largest absolute deviation occurred for the

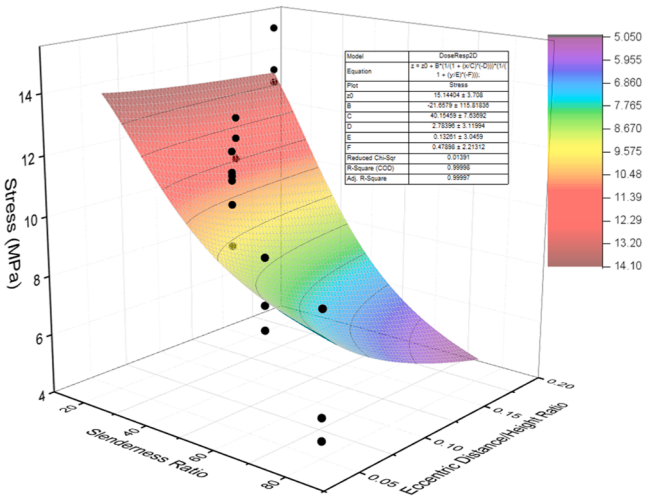

Fig. 18. Spatial fitted curve of the variables.

Table 13
Comparison between proposed formula and the experimental results.

LBL Specimen	Experimental Test Results (kN)	Calculated Results (kN)	Error (%)
LBL 50x50x300	35.04	33.59	4.14
LBL 50x50x450	30.14	28.58	5.18
LBL 50x50x600	27.58	24.20	12.26
LBL 25x25x300	6.78	6.05	10.77
LBL 25x25x450	5.25	4.95	5.71
LBL 25x25x600	4.06	4.73	−16.51

50x50x600 specimen (−3.38 kN), consistent with increased slenderness. For the smaller 25 × 25 series, absolute errors were below 1 kN (−0.73 and −0.30 kN) except for 25x25x600, which showed a small over-prediction (+0.67 kN); its relative error was higher because the capacity was low. Overall error levels were MAE = 1.35 kN and RMSE = 1.69 kN, with a MAPE of 9.09%, supporting the equation's suitability for design-oriented estimation within the tested ranges.

The results presented in Table 13 compare the calculated load-bearing capacities with the experimental test results for various LBL specimens under eccentric compression. The table includes six different specimens with varying cross-sectional dimensions and lengths: LBL50x50x300, LBL50x50x450, LBL50x50x600, LBL25x25x300, LBL25x25x450 and LBL25x25x600. The calculated load-bearing capacities were derived using the proposed formula that incorporates slenderness ratio (λ) and eccentricity/height ratio (e_o/h) as independent variables. The experimental results served as a benchmark to validate the accuracy of the proposed calculation method.

The comparison revealed that the calculated load-bearing capacities closely aligned with the experimental results, with percentage errors ranging from 4.14% to 12.26%. For instance, the LBL50x50x300 specimen had a calculated load-bearing capacity of 33.59 kN, while the experimental result was 35.04 kN, resulting in an error of 4.14%. Similarly, the LBL50x50x450 and LBL50x50x600 specimens showed errors of 5.18% and 12.26%, respectively. The smaller cross-sectional specimens, LBL25x25x300, LBL25x25x450 and LBL25x25x600, exhibited slightly higher errors of 10.77%, 5.71% and −16.51%, respectively. These results show that the proposed calculation method is effective in predicting the load-bearing capacity of LBL columns, particularly for larger cross-sectional specimens. The relatively higher errors observed in the smaller specimens suggest the need for further refinement of the formula to account for the increased sensitivity to geometric and material variability in these columns. Overall, the proposed method demonstrates a promising approach to accurately predicting the load-

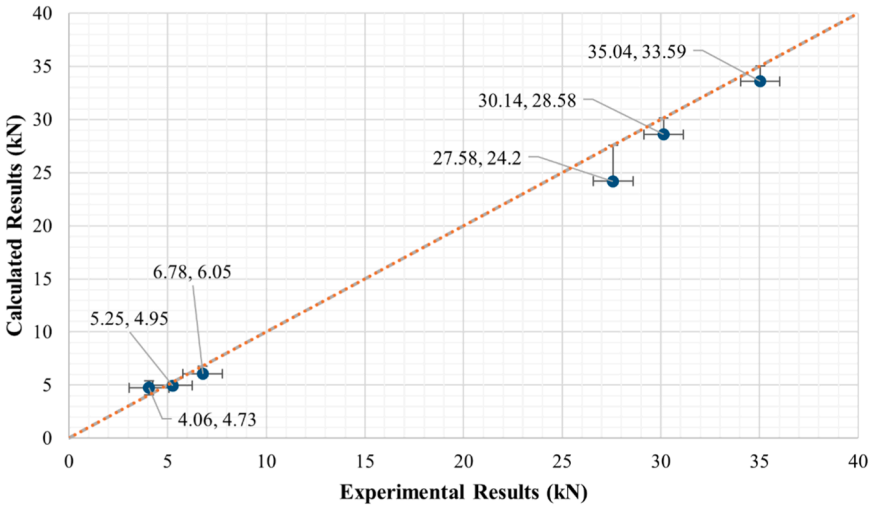

Fig. 19. Experimental vs. calculated ultimate capacity of *B. spinosa* LBL columns.

bearing capacity of LBL columns under eccentric loading conditions.

In this study, a new formula for predicting the ultimate load-bearing capacity of laminated bamboo lumber (LBL) columns was developed, incorporating both slenderness ratio (λ) and eccentricity distance over height ratio (e_o/h) as independent variables. This approach aligns with the methodology used by Zhou et al. (2022), whereas other studies by Li, Liu et al. (2019) and Li, Qiu et al. (2019) considered only the slenderness ratio (λ).

Table 14 provides a comparison of the proposed ultimate load-bearing capacity formula with those in the literature. The R-squared (R^2) values indicate the goodness of fit for each formula, with the proposed formula achieving an R^2 value of 0.95, demonstrating high predictive accuracy. This value is comparable to the R^2 values from other studies, which range from 0.90 to 0.97, indicating that the inclusion of the (e_o/h) ratio provided a significant improvement in the predictive capability of the formula.

According to this dataset, the Li et al., 2019 model attains a slightly lower average error, indicating that its functional form captures the general trend for the specific combinations of (λ) and (e_o/h) tested here. However, the coefficients that Li et al., 2019 obtained were for different LBL systems/species and fabrication routes. The proposed equation, calibrated and validated against *B. spinosa* data, shows a small conservative bias under-prediction) and provides species-appropriate estimates within the stated parameter ranges. We therefore report Li et al. (2019) as an external baseline but recommend the present equation for design use in *B. spinosa* LBL columns within its validity domain.

The actual test results (N_{ul}^t) with the calculated results (N_{ul}^c) using the formulated equations from this study and others are compared in Table 15. The comparison is made to evaluate the accuracy and reliability of the proposed formula. The error percentages, calculated as the difference between the experimental and calculated values, are also presented.

The test results from our study show that the proposed formula provides accurate predictions with error percentages ranging from 4.14% to 16.51%,these error margins are within acceptable limits. Accordingly, the proposed equation is recommended only within the tested parameter range and should be refined as additional experimental data become available. Further work with a larger number of specimens, additional cross-sectional sizes, and broader eccentricity levels is needed to improve the reliability and reduce the prediction error of the model.

Table 14
Comparison of proposed ultimate load bearing capacity calculation.

Author	Formulated ultimate load bearing capacity	R-squared value (R^2)
This study	$N_{ul} = \left\{ 15.1 + \frac{-21.7}{\left[1+\left(\frac{\lambda}{40.2}\right)^{-2.8}\right]\left[1+\left(\frac{\frac{e_o}{h}}{0.1}\right)^{-0.5}\right]} \right\} (A_{LBL})$	0.95
Li et al., 2019	$N_{ul} = 0.029\lambda^2 - 4.72\lambda + 244.37$	0.97
Li et al., 2019	$N_{ul} = 0.0786\lambda^2 - 10.828\lambda + 493.29$	0.94
Zhou et al. (2022)	$N_{ul} = 1.25\lambda^{\left(-0.2016\frac{e_o}{h}-0.3263\right)}\left(\frac{e_o}{h}\right)^{(0.00776\lambda-0.4069)} f_{cu}A$	0.90

Table 15
Actual test results and proposed formula results comparison.

Author	e_o/h	λ	N_{ul}^t (kN)	N_{ul}^c (kN)	Error (%)
This study	0.1667	20.78	35.04	33.59	4.14
	0.1111	31.18	30.14	28.58	5.18
	0.0833	41.57	27.58	24.20	12.26
	0.0833	41.57	6.78	6.05	10.77
	0.0556	62.35	5.25	4.95	5.71
	0.0417	83.13	4.06	4.73	−16.51
Li, Liu et al. (2019)	0.0435	36.8	111.1	110.7	0.4
	0.0336	47.6	82.8	84.3	1.8
	0.0285	56.3	70.7	70.8	0.1
	0.0247	65.0	63.0	61.0	−3.2
	0.0218	73.6	52.7	53.6	1.7
Li, Qiu et al. (2019)	0.0351	20.6	293.3	310.5	5.9
	0.0263	27.4	275	248.9	−9.5
	0.0211	34.3	212.4	207.7	−2.2
	0.0175	41.1	185.7	178.2	−4.0
	0.0150	48.0	144.2	156.0	8.2
	0.0132	54.8	134.3	138.7	3.3
	0.0117	61.7	129.5	124.9	−3.6
	0.0105	68.6	99	113.6	14.7
Zhou et al. (2022)	0.0500	21.1	199.5	217.7	9.1
	0.0273	38.6	128.9	136.8	6.2
	0.0176	59.9	83.5	90.5	8.4
	0.0130	81.0	61.2	64.0	4.5
	0.0100	105.7	43.8	44.6	1.8

5. Conclusions and recommendations

Based on the findings presented in this paper, we successfully investigated the influence of slenderness ratio and eccentricity on the load-bearing capacity of laminated bamboo lumber (LBL) columns derived from *B. spinosa*. Experimental results revealed the inverse relationship between slenderness ratio and stress capacity, highlighting the increased susceptibility to buckling of columns with higher slenderness ratios. Additionally, we demonstrated a direct correlation between eccentricity-to-height ratio and stress capacity, emphasizing the role of eccentric loading in stress concentration.

The proposed empirical equation, incorporating slenderness ratio and eccentricity-to-height ratio, provided reasonable agreement with the experimental results for the tested Bambusa spinosa LBL columns, with MAE = 1.35 kN, RMSE = 1.69 kN, and MAPE = 9.09%. However, comparison with published studies indicates that the error estimates of the present model are higher than those of several existing models. The equation should therefore be regarded as a preliminary species-specific calibration for locally fabricated Bambusa spinosa LBL columns, rather than as a general model with superior predictive accuracy. Additional tests are required to expand the calibration range and reduce model uncertainty.

By addressing the critical interplay of slenderness and eccentricity, this study contributes significant insights into the structural performance of LBL columns and underscores the viability of engineered bamboo as a sustainable construction material. Our findings lay the groundwork for developing design guidelines and advancing the adoption of bamboo in modern construction practices. Based on our findings, a number of recommendations for future research can be made.

Future studies should conduct large-scale experiments to evaluate the behaviour of laminated bamboo lumber (LBL) columns under real-world loading conditions. This would address the limitations of the small-scale specimens that we used, allowing for a more realistic assessment of their structural performance and applicability in full-scale construction projects.

Further research should include more accurate and comprehensive testing configurations to better characterize the physical and mechanical properties of LBL. This should involve advanced testing techniques to capture anisotropic behaviour, adhesive bond performance, and variability across different production batches to improve the reliability of material property data.

The use of Finite Element Analysis (FEA) should be incorporated into future studies to model the complex interactions between slenderness ratio, eccentricity and the material properties of LBL columns. FEA can provide detailed insights into stress distributions, failure modes and the influence of geometric parameters, complementing experimental results and aiding in the refinement of predictive models.

End-region crushing under eccentric load is inherent to the stress gradient at the loaded end. To further de-emphasize local bearing relative to global response in future tests, the load introduction could be refined by (i) slightly increasing bracket contact length, (ii) bonding a thin steel distribution plate (≈1–2 mm) or hardwood pad to spread contact stresses, and (iii) using a spherical seat to minimize incidental misalignment. These measures would preserve the adhesive-based load path and boundary conditions while delaying local crushing.

CRediT authorship contribution statement

Alimuin Patrick Owen Espiritu: Writing – review & editing, Writing – original draft, Investigation, Formal analysis, Conceptualization. **Harvey Ian Aquino:** Visualization, Validation, Supervision. **Dhan Paul Prietos:** Writing – review & editing, Writing – original draft, Visualization, Validation. **Lucena Joe Robert Paul Gacosta:** Writing – review & editing, Investigation, Formal analysis, Data curation. **Manggapis Franklyn Flores:** Writing – review & editing, Writing – original draft, Methodology, Investigation, Formal analysis, Conceptualization. **Carabbacan Aaron Paul Ilao:** Writing – original draft, Visualization, Validation, Methodology, Investigation, Conceptualization. **Kumar Sanjie Dutt Alcala:** Writing – review & editing, Writing – original draft, Supervision, Resources.

Declaration of Competing Interest

The authors declare that they have no known competing financial interests or personal relationships that could have appeared to influence the work reported in this paper

Acknowledgement

The authors would like to express their sincere gratitude and remembrance to the late Engr. Orlean G. Dela Cruz, whose guidance, mentorship, and expertise as thesis adviser were instrumental during the early development of this research. Although he passed away before the completion of the thesis and the subsequent publication of this work, his valuable insights and dedication to engineering education significantly influenced the direction and quality of this study. The authors respectfully acknowledge his lasting contribution and honor his memory through this publication.

Data availability

Data will be made available on request.

References

Amatosa, T.A., Loretero, M.E., Santos, R.B., Giduquio, M.B., 2019. Analysis of sea-water treated laminated bamboo composite for structural application. Nat. Environ. Pollut. Tech. 18 (1), 307–312. ⟨www.neptjournal.com⟩.

Ameh, O.J., Shittu, K.A., 2021. Laminated bamboo board: a sustainable alternative to timber board for building construction. LAUTECH J. Civil. Environ. Stud. 6 (1), 104–115. https://doi.org/10.36108/laujoces/1202.60.0170.

Balasbaneh, A.T., Sher, W., Yeoh, D., Yasin, M.N., 2022. Economic and environmental life cycle perspectives on two engineered wood products: comparison of LVL and GLT construction materials. Environ. Sci. Pollut. Res. 30 (10), 26964–26981. https://doi.org/10.1007/s11356-022-24079-1.

Chen, G., Yu, Y., Li, X., He, B., 2020. Mechanical behavior of laminated bamboo lumber for structural application: an experimental investigation. Eur. J. Wood Wood Prod. 78 (1), 53–63. https://doi.org/10.1007/s00107-019-01486-9.

Eberhardt, L., Birgisdottir, H., Birkved, M., 2019. Comparing life cycle assessment modelling of linear vs. circular building components. IOP Conf. Series Earth Environmental Science 225, e012039. https://doi.org/10.1088/1755-1315/225/1/012039.

Hao, M., Chang, W., Xu, C., 2024. Failure modes determination and load-bearing capacity evaluation of concrete columns under seismic loads by ANNs. Soft Comput. 28 (13–14), 8361–8377. https://doi.org/10.1007/s00500-024-09741-9.

Hong, C., Li, H., Xiong, Z., Lorenzo, R., Corbi, I., Corbi, O., 2021. Experimental and numerical study on eccentric compression properties of laminated bamboo columns with a chamfered section. J. Build. Eng. 43, e102901. https://doi.org/10.1016/j.jobe.2021.102901.

Huang, D., Bian, Y., Huang, D., Zhou, A., Sheng, B., 2015. An ultimate-state-based-model for inelastic analysis of intermediate slenderness PSB columns under eccentrically compressive load. Constr. Build. Mater. 94, 306–314. https://doi.org/10.1016/j.conbuildmat.2015.06.059.

Iroegbu, A., Ray, S., 2021. Bamboos: From bioresource to sustainable materials and chemicals. Sustainability 13 (21), e12200. https://doi.org/10.3390/su132112200.

Jian, B., Li, H., Zhou, K., Ashraf, M., Xiong, Z., Zheng, X., 2023. Mechanical evaluation on BFRP laminated bamboo lumber columns under eccentric compression. Adv. Struct. Eng. 26 (5), 809–823. https://doi.org/10.1177/13694332221138312.

Li, H., Chen, G., Zhang, Q., Ashraf, M., Xu, B., Li, Y., 2016. Mechanical properties of laminated bamboo lumber column under radial eccentric compression. Constr. Build. Mater. 121, 644–652. https://doi.org/10.1016/j.conbuildmat.2016.06.031.

Li, H., Liu, R., Lorenzo, R., Wu, G., Wang, L., 2019. Eccentric compression properties of laminated bamboo columns with different slenderness ratios. In: Proceedings of the Institution of Civil Engineers - Structures and Buildings, 172, pp. 315–326. https://doi.org/10.1680/jstbu.18.00007.

Li, H., Qiu, Z., Wu, G., Corbi, O., Wei, D., Wang, L., Corbi, I., Yuan, C., 2019. Slenderness ratio effect on eccentric compression properties of parallel bamboo strand lumber columns. J. Struct. Eng. 145 (8). https://doi.org/10.1061/(ASCE)ST.1943-541X.0002372.

Li, H., Su, J., Xiong, Z., Ashraf, M., Corbi, I., Corbi, O., 2020. Evaluation on the ultimate bearing capacity for laminated bamboo lumber columns under eccentric compression. Structures 28, 1572–1579. https://doi.org/10.1016/j.istruc.2020.10.004.

Liu, S., Gao, D., Xie, Y., Chen, B., 2022. Experimental study and theoretical analysis of side-pressure laminated bamboo lumber columns under axial compression. Sustainability 14 (18), e11360. https://doi.org/10.3390/su141811360.

Lucena, J.R.P.G., Dela Cruz, O.G., 2023. A literature review on the use of bamboo as a truss member and fiber-reinforced polymer as a truss jointing material. Int. J. Integr. Eng. 15 (2), 172–185. https://doi.org/10.30880/ijie.2023.15.02.017.

Manggapis, F.F., Dela Cruz, O.G., 2024. An in-depth review on the eccentric compression performance of engineered bamboo columns. Civil. Eng. J. 10 (3), 974–993. https://doi.org/10.28991/cej-2024-010-03-020.

Salzer, C., Wallbaum, H., Alipon, M., Lopez, L.F., 2017. Determining material suitability for low-rise housing in the Philippines: physical and mechanical properties of the bamboo species *Bambusa blumeana*. BioResources 13 (1), 346–369. https://doi.org/10.15376/biores.13.1.346-369.

Soni, A., Das, P.K., Hashmi, A.W., Yusuf, M., Kamyab, H., Chelliapan, S., 2022. Challenges and opportunities of utilizing municipal solid waste as alternative building materials for sustainable development goals: a review. Sustain. Chem. Pharm. 27, e100706. https://doi.org/10.1016/j.scp.2022.100706.

Wang, Y., Li, H., Yang, D., Liu, K., Yuan, C., Corbi, O., 2023. Mechanical properties of bolted steel laminated flattened-bamboo lumber connections under cyclic loading. Constr. Build. Mater. 385, e131511. https://doi.org/10.1016/j.conbuildmat.2023.131511.

Wang, C., Zhang, H., Zhao, C., Zhang, C., Cao, T., Dong, H., Ding, J., Xiong, Z., Xiong, X., Liu, W., Wu, K., Liu, R., Ding, W., Yan, Z., 2018. Experimental study on laminated bamboo lumber column. E3S Web Conf. 38, e02001. https://doi.org/10.1051/e3sconf/20183802001.

Yan, B., Zhou, X., Liu, J., 2019. Behavior of circular tubed steel-reinforced-concrete slender columns under eccentric compression. J. Constr. Steel Res. 155, 342–354. https://doi.org/10.1016/j.jcsr.2018.11.018.

Yang, D., Li, H., Xiong, Z., Mimendi, L., Lorenzo, R., Corbi, I., Corbi, O., Hong, C., 2020. Mechanical properties of laminated bamboo under off-axis compression. Compos. Part A Appl. Sci. Manuf. 138, e106042. https://doi.org/10.1016/j.compositesa.2020.106042.

Zhou, K., Li, H., Dauletbek, A., Yang, D., Xiong, Z., Lorenzo, R., Zhou, K., Corbi, I., Corbi, O., 2022. Slenderness ratio effect on the eccentric compression performance of chamfered laminated bamboo lumber columns. J. Renew. Mater. 10 (1), 165–182. https://doi.org/10.32604/jrm.2021.017223.